CHARGED PARTICLE CONFINEMENT IN MAGNETIC MIRROR

D. BORA, P.I. JOHN, Y.C. SAXENA, R.K. VARMA
Physical Research Laboratory,
Ahmedabad, India

Abstract:

The behavior of single charged particle trapped in a magnetic mirror has been investigated experimentally. The particle injected off axis and trapped in a magnetic mirror, leak out of the mirror with the leakage characterised by multiple decay times. The observed decay times, are in good agreement with predictions of a "wave mechanical like" model by Varma, over a large range of relevant parameters.

1. Introduction:

Study of behavior of charged particles in a magnetic confinement system still draws considerable interest. The renewed interest in this problem is due to its importance from the point of view of design considerations of large machines as the nonadiabaticity of the magnetic moment constitutes another mechanism for the loss of particles from a magnetic mirror. The experimental results often deviate from the adiabatically predicted theoretical values. There have been single particle experiments to study the deviations in the behaviour of charged particles from the adiabatic theory in a magnetic mirror [1,2,3] . Our recent experiments have clearly demonstrated the existence of distinct multiple life times for the leakage of charged particles injected off axis with same initial energy and magnetic moment [4,5] . These results are in qualitative agreement with the "wave mechanical like" model for the leakage of charged particles from a magnetic barrier [6] . These experiments were, however carried out on the particles injected into the mirror at pitch angles close to but greater than the loss cone angle of the mirror. The calculations based on the model [6] indicate that the results are very sensitive to the exact value of the pitch angle for ang les close to the loss cone angle. The experiments have therefore been repeated with particles injected at a larger pitch angle. In order to check the range of validity of the model the experiments have also been conducted on particles injected at different radial positions and at different particle densities. The magnetic field configuration has also been altered and the experiment performed for such varied conditions. These results are presented in the following.

2. Experimental System.

The schematic of the experimental system is shown in Fig. 1a. The stainless steel experimental chamber is evacuated to a pressure of $\sim 5 \times 10^{-8}$ Torr. The electron gun, placed at one end of the system acts as the source of charged particle. The particles are injected at pitch angles $\theta \simeq 35^{\circ}$ and 33°. Due to the physical dimension of the system, it was not possible to inject the particles at higher pitch angles. The magnetic field coils placed at different axial positions together generated the desired static magnetic field profiles which are shown in fig. 1b. Different field profiles were generated by adjusting the axial position of the coils or by adjusting the current passing through different coils. In these cases, to reduce the current through certain coils, shunts of low resistance and high current rating in the form of stainless steel strips of different thickness, width and length are used. The field configurations are numerically calculated following a minimisation scheme.

For effective confinement of the charged particles, the injected particles must be made to feel some change in the parameters of the experimental system. For this purpose, the magnetic field value at the mirror throat near the injection point is lowered during injection. To confine the electrons, the magnetic field value at the mirror throat at the injection end is raised to its initial value equal to the value at the other mirror point before the reflected electrons approach the mirror. This is achieved by means of pulsed magnetic field superimposed on the static magnetic field at the mirror throat. Pulsed current is fed to a small coil placed near the source. To form this high current rectangular pulse, a coaxial cable terminated with its characteristic impedance is used.

The required pulse duration and the magnitude of the field value used are dependent on the energy of the electron beam. Since minimum dispersion in the beam energy is desired, sufficient care is taken while constructing the pulse

forming network. A 100 amp current pulse of 150 nsec duration with a fall time of 30 nsec is used to produce the pulsed magnetic field. Fig.2(a) shows the trace from an oscillogram of the current pulse registered with the help of a current transformer (Pearson model no.411). The magnetic field produced by this current is measured with the help of a magnetic probe. Fig.2(b) is a signal registered with the help of the magnetic probe.

A low current electron gun is used for the experiment. The energy of the electrons can be varied upto 5 kev with a beam current of 0.2 –0.4 μA. Since the experiment dealt with single particle phenomena, the density of the beam is kept low, typically of the order of 10^4 particles/cc. The beam pulse duration is 30 nsec. To form the pulsed beam a grid is placed infront of the cathode and the grid is kept at negative potential along with the cathode with respect to the accelerating electrodes. A 300 V pulse with 30 nsec duration is applied to the cathode making the grid 300 V positive with respect to the cathode. During this time a pulse of electrons escapes through the grid and is accelerated through the cylindrical electrodes.

An electrostatic analyzer placed outside the mirror throat is used to measure the current due to the leakage of the particles. This signal is fed to the current to voltage converter, the inverted output is logarithmically amplified, digitized by means of an A/D converter and then recorded on a digital tape recorder. Recorder data is analysed with the help of IBM 360 computer. The digitization error for the signal was ~1 %.

The radial position of the source can be varied with the help of an Ultra High Vacuum feed through. The source is placed about 11 cm away from the mirror throat.

3. Results and Discussion:

The semilog plot of leakage current as a function of time for different magnetic field values does not represent a straight line. This suggests the existence of more than one life time characterising the decay curve. To see if this indeed is the case and to determine the life times, the signal is analysed in terms of a sum of exponentials with different e folding times and amplitudes. The life times (τ_n) thus obtained, are measured as a function of magnetic field

strength for different energy of particles and different pitch angles. $\ln \tau_n$ values are plotted as a function of different magnetic field values for different energy of the particles and different magnetic field scale lengths. The slope values (m_n) thus obtained is compared with the theoretically obtained slope values. The m_n can be written as

$$m_n = \sqrt{2m}\,\frac{2\pi e n}{mc\alpha\sqrt{E}}\left\{\left(\frac{B_m}{B}-\frac{B_o}{B}\right)^{1/2}\sin\theta-\left(1-\sin^2\theta\,\frac{B_o}{B}\right)^{1/2}\right\}$$

It is seen that the slope values corresponding to different life times vary as multiple integers of the lowest.

As reported earlier [7] it is observed that the ratio (m_2/m_1) has value close to 2 and the scatter of the values around the theoretically predicted value of 2 is smaller for larger pitch angle than for the smaller pitch angle.

Using the experimental slope values, pitch angle values were calculated and are tabulated in table I. The extent of this range is smaller than the previous results. This suggests a decrease in sensitivity of the slope on the pitch angle as one moves away from the adiabatic loss cone angle.

To see the radial dependence of the slope values, the source is shifted radially with the help of an Ultra High Vacuum feed through. The life time variation as a function of the magnetic field is measured at four different radial positions. The slope values obtained for the two lifetimes alongwith their ratios are tabulated in table II. The slope values increase as the source is moved radially outward. It was observed that the second life time for the charged particles increased sharply as a function of magnetic field values for radially inner positions. However, the first lifetime did not show any tendency of saturation at these magnetic field values. The homogeneity in the radial magnetic field is of the order of 80 % over a radius of 4 cm around the axis of symmetry.

The density of the beam is varied by varying the emission current at the source. However, higher emission currents spoil the UHV conditions, thereby limiting the beam currents upto $I_b \simeq 1.5\ \mu$A. Table III shows the slope values (m_1, m_2) and the ratio of the slope values m_2/m_1 for three different beam currents keeping the initial energy, magnetic field scale length and the pitch angle constant. Within

this range of variation of the beam current, the ratio of the slope values lie within the range 1.7 to 2.08.

In general, two decay times with different fractional amplitudes can be fitted through the curves. However, in certain cases, the fit is better for three life times. Fig.3 shows a semilog plot of the three time scales as a function of the maximum magnetic field. The time scales alongwith the amplitude values are tabulated in table IV. It is seen that error levels on the amplitudes corresponding to third life time are significantly large . However, the ratio of the slopes of these curves is 1:2.3:3.2, in good agreement with the theoretical model.

In the theoretical model [6] the magnetic field configurations near the mirror region has been represented by the potential of the form $\mu\Omega_{max}\,\mathrm{sech}^2(\alpha z)$ where μ – action of the particle, Ω_{max} — cyclotron frequency at the maximum magnetic field, while the configuration used in experiment is different (narrower, as shown in fig.1). Experiments have also been carried out for a magnetic configuration close to the one assumed theoretically. The $\ln \tau_n$ vs B curve for this particular configuration is plotted in fig.5 for E=2.2 kev, α^{-1} = 9 cm and $\theta \simeq 33^{\circ}$. The experimental slope values for such a potential are compared with the slope values for E=2.2 kev and α^{-1} = 8 cm for the previous field configuration (of fig. 1) and are found to be larger by a factor of about four. The ratio of slopes corresponding to the second and first life time in this case is found to be 2.3.

4. Conclusions:

In the range of variations of different parameters of the system, two life times are distinctly observed. Three decay times were observed for some experimental parameters. Although the ratio of the slopes are in agreement with the theoretical predictions, the error bars on the values of the third decay time and corresponding amplitudes are large.

REFERENCES.

[1] Balebanov V. M and Semashko N. N, Nucl. Fus. 7, 207 (1967).

[2] Dubinina A. N; Krasitskaya L. S and Yudin Yu. N; Plasma Phys. II, 551 (1969)

[3] Ponomarenko V. G; Tranin L. Ya; Yurchenko V. I and Yasnetskii A. N; Sov. Phys. JETP, 23, 1, (1969).

[4] Bora D; John P. I; Saxena Y. C; Varma R. K; Phys. Lett. 75A, 60 (1979).

[5] Bora D; John P. I; Saxena Y. C; Varma R. K. ; Plasma Phys. 22, 563 (1980).

[6] Varma R. K; Phys. Rev. Lett. 26, 417, (1971).

[7] Bora D; John P. I; Saxena Y. C; Varma R. K.; Proceedings of International Conf. on Plasma Phys; Nagoya; Japan, 7P II 26 (1980).

Table I.

THEORETICALLY CALCULATED VALUES OF THE PITCH ANGLE.

Sl. No.	E (Kev)	α^{-1} (cm)	$m_1 \times 10^{-3}$	θ° (theoretical.)
1	2.2	8	5.56 ± .18	34° 19' 57"
2	2.9	8	4.9 ± .24	34° 21' 12"
3	3.7	8	4.54 ± . 3	34° 21' 12"
4	4.5	8	3.96 ± .42	34° 20' 20"
5	2.9	11	6.16 ± .18	34° 18' 22"
6	2.9	13	8.24 ± . 3	34° 20' 56"

Table II.

SLOPE VALUES FOR DIFFERENT RADIAL POSITIONS

E = 2.2 Kev; α^{-1} = 8 cm ; θ = 35°			
r (cm)	$m_1 \times 100$	$m_2 \times 100$	m_2/m_1
1.8	0.42 ± 0.02	0.71 ± 0.03	1.7
2.2	0.55 ± 0.07	1.02 ± 0.18	1.8
3.0	0.56 ± 0.02	1.19 ± 0.05	2.14
3.5	0.86 ± 0.08	1.47 ± 0.04	1.7

Table III

SLOPE VALUES FOR DIFFERENT BEAM CURRENTS

E = 2.2 Kev ; α^{-1} = 8 cm ; θ = 33°; r = 3 cm			
I (μA)	$m_1 \times 100$	$m_2 \times 100$	m_2/m_1
0.16	0.10 ± 0.01	0.18 ± 0.07	1.75
0.66	0.33 ± 0.07	0.35 ± 0.04	1.70
1.30	0.26 ± 0.02	0.54 ± 0.04	2.10

Table IV

TIME SCALE AND AMPLITUDE FOR THREE LIFE TIMES

E = 3.7 Kev ; α^{-1} = 8 cm ; θ = 33°			
B(Gauss)	T_1 (m Sec)	T_2 (m Sec)	T_3 (m Sec)
270	0.227	0.475	0.823
335	0.236	0.514	0.954
400	0.242	0.585	1.060
470	0.255	0.628	1.150
540	0.262	0.647	1.300
B(Gauss)	A_1 (%)	A_2 (%)	A_3 (%)
270	75 ± 12	30 ± 4	5 ± 2.0
335	67 ± 8	26 ± 5	2.3 ± 2.0
400	70 ± 9	26 ± 6	2.5 ± 2.0
470	67 ± 8	27 ± 5	3.7 ± 2.0
540	74 ± 11	26 ± 5	2.3 ± 1.5

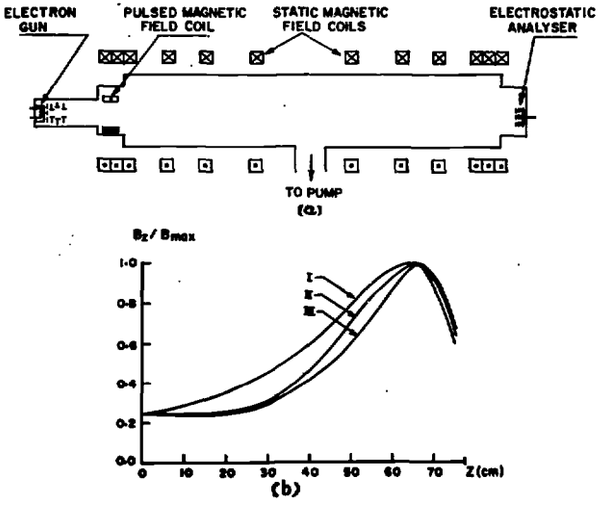

Fig. 1: (a) Schemetic of the experimental system. (b) Axial distribution of magnetic field (from the centre of the system to one mirror end) for different scale lengths (I) 13 cm (II) 11 cm and (III) 8 cm.

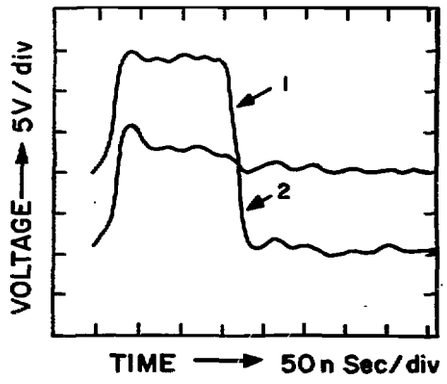

Fig. 2: Current pulse shape (1) and the shape of resulting magnetic field (2).

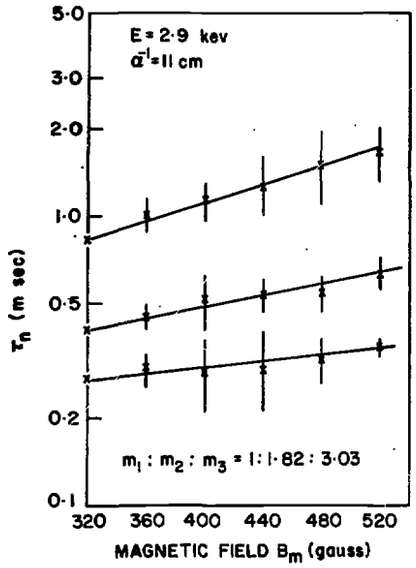

Fig. 3: Three life times as function of the maximum magnetic field B_m at the mirror throat.

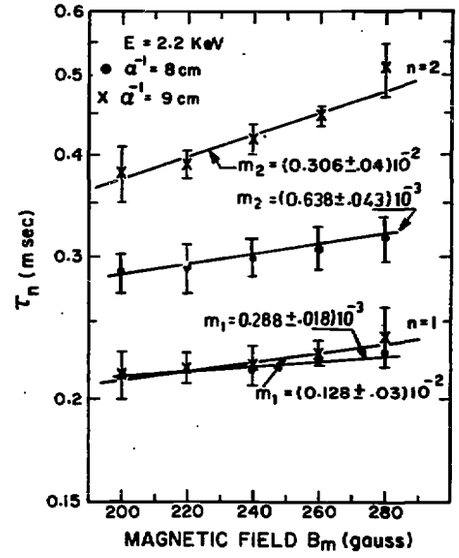

Fig. 4: Dependence of the life times on the magnetic field for two different shapes of the field at mirror throat.